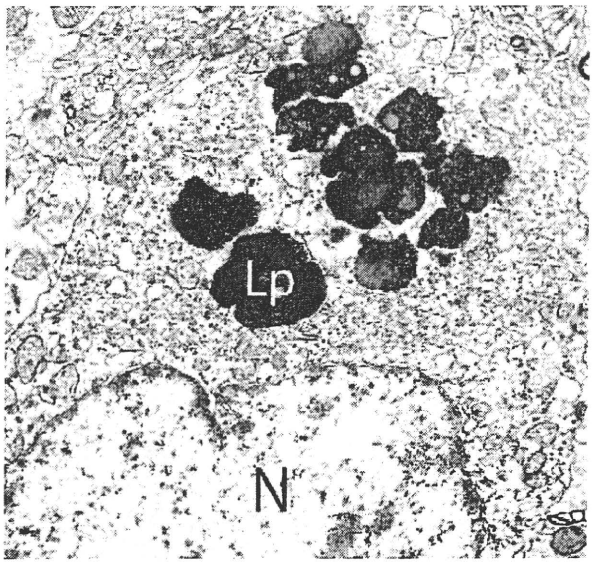

Fig. 3 Routine electron-microscopic ultrathin section adjacent to that in Figure 2. The ubiquitin-positive area seems to consist of ordinary cytoplasmic organelles, with a few filaments. Ribosome-like granules are less electron-dense and more irregular, with amorphous outlines, than the ribosomes in the non-ubiquitinated cytoplasmic area, ×3.3 (original). N, nucleus; Lp, lipofucin.

the area (Fig. 3). The area seemed to consist of ordinary cytoplasmic organelles, including lipofuscin, mitochondria, cytoplasmic reticulum, and many ribosome-like granules. There were a few filamentous structures. When the findings from immunoelectron-microscopic and semithin sections were compared, the ubiquitin-positive structures seemed to correspond to ribosome-like granules and filaments. The granules were less electron-dense and more irregular, with amorphous outlines, than the ribosomes in the non-ubiquitinated cytoplasm. These findings suggest the development of ribosome-associated and ubiquitin-related abnormalities in the neurons of the extra-motor cortices of these patients.

NATURE OF THE INCLUSIONS

The inclusions were positive for ubiquitin-binding protein p62[12,13] and vacuole-creating protein.[14] However, their main components were unknown. In 2006, Neumann *et al.*[15] and Arai *et al.*[16] found that the ubiquitin-positive tau-negative inclusions are composed of the 43-kDa TAR DNA-binding protein (TDP-43). Diseases that include TDP-43-positive inclusions have recently been classified as TDP-43 proteinopathy.[17]

ACKNOWLEDGMENTS

This work was supported by Grants-in-Aid from the Ministry of Health, Labour and Welfare of Japan, and also from the Ministry of Education, Culture, Sports, Science and Technology of Japan.

REFERENCES

1. Yuasa R. Amyotrophic lateral sclerosis with organic dementia: report a case. *Clin Neurol* 1964; **4**: 529–534.
2. Mitsuyama Y. Presenile dementia with motor neuron disease in Japan: clinicopathological review of 26 cases. *J Neurol Neurosurg Psychiatry* 1984; **47**: 953–959.
3. Tanaka M, Okamoto K. The spectrum of cognitive dysfunction in ALS/MND in the Japanese population. In: Strrong MJ, ed. *Dementia and Motor Neuron Disease.* London: Informa, 2006; 73–85.
4. Okamoto K, Hirai S, Shoji M, Harigaya Y, Yamaguchi H, Takatama M. Senile changes in amyotrophic lateral sclerosis. *Neurobiol Aging* 1990; **11**: 274.
5. Okamoto K, Hirai S, Yamazaki T, Sun X, Nakazato Y. New ubiquitin-positive intraneuronal inclusions in the extra-motor cortices in patients with amyotrophic lateral sclerosis. *Neurosci Lett* 1991; **129**: 233–236.
6. Okamoto K, Murakami N, Kusaka H *et al.* Ubiquitin-positive intraneuronal inclusions in the extramotor cortices of presenile dementia patients with motor neuron disease. *J Neurol* 1992; **239**: 426–430.
7. Wightman G, Anderson VER, Martin J *et al.* Hippocampal and neocortical ubiquitin-immunoreactive inclusions in amyotrophic lateral sclerosis with dementia. *Neurosci Lett* 1992; **139**: 269–274.
8. The Lund and Manchester Groups. Clinical and neuropathological criteria for frontotemporal dementia. *J Neurol Neurosurg Psychiatry* 1994; **57**: 416–418.
9. Neary D, Snowden JS, Gustafson L *et al.* Frontotemporal lobar degeneration. A consensus on clinical diagnostic criteria. *Neurology* 1998; **51**: 1546–1554.
10. McKhann GM, Albert MS, Grossman M, Miller B, Dickson D, Trojanowski JQ. Clinical and pathological diagnosis of frontotemporal dementia. Report of the work group on frontotemporal dementia and Pick's disease. *Arch Neurol* 2001; **58**: 1803–1809.
11. Okamoto K, Hirai S, Amari M. Electron micrograph of ubiquitin-positive intraneuronal inclusions in the extra-motor cortices of amyotrophic lateral sclerosis. *Neuropathology* 1996; **16**: 112–116.
12. Arai T, Nonaka T, Hasegawa M *et al.* Neuronal and glial inclusions in frontotemporal dementia with or without motor neuron disease are immunopositive for p62. *Neurosci Lett* 2003; **342**: 41–44.
13. Nakano T, Nakaso K, Nakashima K, Ohama E. Expression of ubiquitin-binding protein p62 in ubiquitin-immunoreactive intraneuronal inclusions in amyotrophic lateral sclerosis with dementia: analysis of

five autopsy cases with broad clinicopathological spectrum. *Acta Neuropathol* 2004; **107**: 359–364.
14. Mizuno Y, Hori S, Kakizuka A, Okamoto K. Vacuole-creating protein in neurodegenerative disease in humans. *Neurosci Lett* 2003; **343**: 77–80.
15. Neumann M, Sampathu DM, Kwong LK *et al.* Ubiquitinated TDP-43 in frontotemporal lobar degeneration and amyotrophic lateral sclerosis. *Science* 2006; **314**: 130–133.
16. Arai T, Hasegawa M, Akiyama H *et al.* TDP-43 is a component of ubiquitin-positive tau-negative inclusions in frontotemporal lobar degeneration and amyotrophic lateral sclerosis. *Biochem Biophys Res Commun* 2006; **351**: 602–611.
17. Cairns NJ, Bigio EH, Mackenzie IRA *et al.* Neuropathologic diagnosis and nosologic criteria for frontotemporal lobar degeneration: consensus of the Consortium for Frontotemporl Lobar Degeneration. *Acta Neuropathol* 2007; **114**: 5–22.

The British Journal of Radiology, 84 (2011), 229–235

Comparison of pulmonary thin section CT findings and serum KL-6 levels in patients with sarcoidosis

[1]K HONDA, MD, [1]F OKADA, MD, [1]Y ANDO, MD, [1]H MORI, MD, [2]K UMEKI, MD, [2]H ISHII, MD, [2]J KADOTA, MD, [3]M ANDO, MD, [3]E MIYAZAKI, MD and [3]T KUMAMOTO, MD

Departments of [1]Radiology, [2]Internal Medicine II and [3]Internal Medicine III, Oita University Faculty of Medicine, Oita, Japan

Objective: This study aimed to compare thin-section CT images from sarcoidosis patients who had either normal or elevated serum KL-6 levels.
Methods: 101 patients with sarcoidosis who underwent thin-section CT examinations of the chest and serum KL-6 measurements between December 2003 and November 2008 were retrospectively identified. The study group comprised 75 sarcoidosis patients (23 male, 52 female; aged 19–82 years, mean 54.1 years) with normal KL-6 levels (152–499 U ml^{-1}, mean 305.7 U ml^{-1}) and 26 sarcoidosis patients (7 male, 19 female; aged 19–75 years, mean 54.3 years) with elevated KL-6 levels (541–2940 U ml^{-1}, mean 802.4 U ml^{-1}). Two chest radiologists, unaware of KL-6 levels, retrospectively and independently interpreted CT images for parenchymal abnormalities, enlarged lymph nodes and pleural effusion.
Results: CT findings in sarcoidosis patients consisted mainly of lymph node enlargement (70/75 with normal KL-6 levels and 21/26 with elevated KL-6 levels), followed by nodules (50 and 25 with normal and elevated levels, respectively) and bronchial wall thickening (25 and 21 with normal and elevated levels, respectively). Ground-glass opacity, nodules, interlobular septal thickening, traction bronchiectasis, architectural distortion and bronchial wall thickening were significantly more frequent in patients with elevated KL-6 levels than those with normal levels ($p<0.001$, $p<0.005$, $p<0.001$, $p<0.001$, $p<0.001$ and $p<0.001$, respectively). By comparison, there was no significant difference in frequency of lymph node enlargement between the two groups.
Conclusion: These results suggest that serum KL-6 levels may be a useful marker for indicating the severity of parenchymal sarcoidosis.

Received 26 July 2009
Revised 17 September 2009
Accepted 6 October 2009

DOI: 10.1259/bjr/65287605

KL-6 is a mucin-like high molecular weight glycoprotein that is expressed on Type II pneumocytes and respiratory bronchiolar epithelial cells in the normal lung [1, 2]. Serum levels of KL-6 are elevated in various respiratory and non-respiratory conditions, including breast and pancreatic cancers [3, 4] and diabetes mellitus [5]. This observation has led to a focus on the use of KL-6 as a diagnostic and prognostic tool in respiratory diseases.

Serum and bronchoalveolar lavage fluid levels of KL-6, first described by Kohno et al [6] in 1988, were raised in patients with interstitial pneumonia [1, 2, 7]. Several investigators have also reported that KL-6 is a useful serum marker to confirm diagnosis and for long-term management in patients with diffuse pulmonary diseases, particularly interstitial lung diseases. Patients with idiopathic pulmonary fibrosis or non-specific interstitial pneumonia showed significantly elevated KL-6 levels [8–13].

Several studies indicate that the serum KL-6 level is elevated in patients with sarcoidosis [14–16]. However, no studies describing radiological findings comparing thin-section CT images between patients with elevated KL-6 levels and those with normal KL-6 levels have been published in the English language literature.

Address correspondence to: Dr Fumito Okada, Department of Radiology, Oita University Faculty of Medicine, Oita, Japan, 1-1 Idaigaoka, Hasama-machi, Yufu, Oita 879-5593, Japan. E-mail: fumitook@med.oita-u.ac.jp

Thus, we aimed to retrospectively evaluate and compare pulmonary CT findings between patients with elevated KL-6 levels and those with normal KL-6 levels.

Methods and materials

Patients

101 patients with known serum KL-6 levels who underwent thin-section CT between December 2003 and November 2008 at our institutions, and in whom sarcoidosis was histologically and clinically diagnosed, were included in this study. Thin-section CT scans were performed within 3 days of KL-6 level measurements. Transbronchial lung biopsy and other tissue biopsies were performed within 2 weeks of the CT scan.

Our study included 75 sarcoidosis patients (23 men, 52 women; age range 19–82 years; mean age 54.1 years) with normal KL-6 levels (152–499 U ml^{-1}; mean 305.7 U ml^{-1}; Table 1) in whom transbronchial lung biopsy (n=42), surgical lung biopsy (n=1), lymph node biopsy (n=12), muscle biopsy (n=4), testis biopsy (n=1), skin biopsy (n=5) or clinical diagnosis (n=10) had been performed. 26 sarcoidosis patients (7 men, 19 women; age range 19–75 years; mean age 54.3 years) with elevated KL-6 levels (521–2940 U ml^{-1}; mean 802.4 U ml^{-1}; Table 1) in

Table 1. Comparison of thin-section CT findings

Finding	Normal KL-6 (n=75)	Elevated KL-6 (n=26)	p-Value
Consolidation	3 (4.0)	2 (7.7)	NS
Ground-glass opacity	10 (13.3)	16 (61.5)	<0.001
Nodules	50 (66.7)	25 (96.2)	<0.005
Interlobular septal thickening	20 (26.7)	25 (96.2)	<0.001
Traction bronchiectasis	7 (9.3)	25 (96.2)	<0.001
Intralobular reticular opacity	3 (4.0)	0 (0)	NS
Architectural distortion	7 (9.3)	26 (100)	<0.001
Bronchial wall thickening	25 (33.3)	21 (80.8)	<0.001
Lymph node enlargement	70 (93.3)	21 (80.8)	NS
Pleural effusion	0 (0)	0 (0)	NS

Data in parentheses are percentages. NS, not significant.

whom transbronchial lung biopsy (n=18), lymph node biopsy (n=4), muscle biopsy (n=1), liver biopsy (n=1) or clinical diagnosis (n=2) had been performed were also included in this study. The ethical review boards of the institutions that contributed cases to this study did not require approval or informed consent for the retrospective review of patient records and images.

Patients with idiopathic interstitial pneumonia were excluded from the study. Moreover, patients with all other known cases of interstitial pneumonia (*i.e.* connective tissue disease, pneumoconiosis, hypersensitivity pneumonitis or drug-induced pneumonitis), those diagnosed with concurrent infectious diseases by serological tests and by clinical and pathological findings, and those with malignancy or diabetes mellitus were excluded.

Sarcoidosis was diagnosed on the basis of histological findings and clinical history. The clinical findings in all patients were subsequently reviewed by two chest radiologists to ensure that all cases fulfilled the diagnostic criteria recommended by the American Thoracic Society and the European Respiratory Society [17].

CT examinations

Thin-section CT examinations were performed within 7 days of the chest radiographs. The CT examinations were performed with 1 mm collimation at 10 mm intervals from the apex of the lung to the diaphragm (n=25; 19 with normal KL-6 levels and 6 with elevated KL-6 levels), or volumetrically with a multidetector CT system with 1 mm reconstruction (n=76; 56 with normal KL-6 levels and 20 with elevated KL-6 levels). CT images were obtained at the end of inspiration and in a supine position. The scanning protocol consisted of the reconstruction of 1 mm collimation sections with a high spatial frequency algorithm at 10 mm intervals. Images were captured at window settings allowing the viewing of the lung parenchyma (window level −600 to −700 HU; window width 1200–1500 HU) and the mediastinum (window level 20–40 HU; window width 400 HU). All initial scans were evaluated.

Radiographic interpretation

Images were reviewed independently, in a random order, by two chest radiologists (with 21 and 9 years of experience in chest image interpretation). The observers were unaware of KL-6 levels and clinical information.

Chest radiographs were used to classify the patients as being Type 0 (normal chest radiograph), Type I (bilateral hilar lymphadenopathy), Type II (bilateral hilar lymphadenopathy with pulmonary infiltrates) and Type III (pulmonary infiltrates without lymphadenopathy).

CT images were assessed for the following radiological patterns: ground-glass opacity, consolidation, nodules, interlobular septal thickening, traction bronchiectasis, intralobular reticular opacity, architectural distortion, bronchial wall thickening, enlarged hilar/mediastinal lymph node(s) (>1 cm in diameter of the short axis) and pleural effusion. Areas of ground-glass opacity were defined as hazy increases in attenuation without obscuration of vascular markings [18, 19]. Areas of consolidation were defined as areas of increased attenuation causing obscuration of normal lung markings [18, 19]. Interlobular septal thickening was defined as abnormal widening of interlobular septa [19]. Intralobular reticular opacity was considered present when interlacing line shadows were separated by a few millimetres [18, 19]. Traction bronchiectasis was defined as irregular bronchial dilatation within the surrounding areas showing parenchymal abnormalities. Architectural distortion was considered present when bronchi, pulmonary vessels or interlobular fissures or septa were abnormally displaced [19].

Measurement of KL-6 levels

Serum KL-6 levels were measured within 3 days of the initial CT scans and before steroid treatment using a sandwich-type enzyme-linked electrochemiluminescence immunoassay kit (Picolumi KL-6; Sanko Junyaku, Tokyo). The recommended cut-off value was determined at 500 U ml^{-1} according to levels reported in healthy individuals [6]. The assay was performed by technicians unaware of the clinical information related to the samples.

Statistical analysis

Statistical analyses of the incidence of symptoms and laboratory data were conducted using Fisher's exact test and the χ^2 test. Mean age comparison was conducted using Student's t-test. A $p<0.05$ was considered to be statistically significant.

Results

Radiographs

Patients were radiographically classified as being Type 0 (n=17), Type I (n=29), Type II (n=38) or Type III (n=17). The mean KL-6 value was 301±244 U ml^{-1} in stage 0, 333±259 U ml^{-1} in stage I, 1136±777 U ml^{-1} in stage II and 1331±775 U ml^{-1} in stage III. The serum

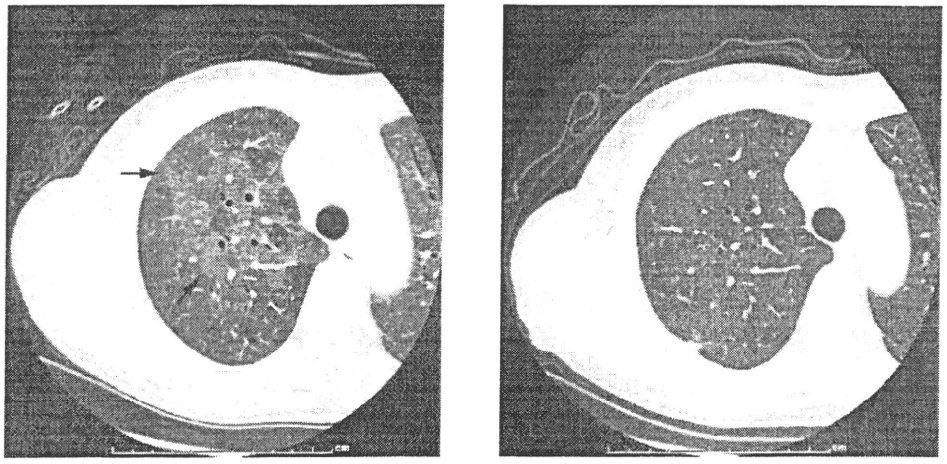

(a) (b)

Figure 1. Images in a 69-year-old woman. (a) Transverse CT scan (1 mm section thickness) obtained at the level of right upper lobe shows ground-grass appearance (arrows; KL-6, 2940 U ml^{-1}). (b) Transverse CT scan (1 mm section thickness) obtained, after surgical biopsy 4 years later, shows disappearance of ground-grass opacity (KL-6, 313 U ml^{-1}).

KL-6 levels for Type II or III were significantly elevated compared with those in Type 0 and I ($p<0.01$).

CT patterns

CT findings are summarised in Table 1. Of the 75 patients with normal KL-6 levels, nodules ($n=50$, 66.7%) were observed most frequently, followed by bronchial wall thickening ($n=25$, 33.3%), interlobular septal thickening ($n=20$, 26.7%), ground-glass opacity ($n=10$, 13.3%), architectural distortion ($n=7$, 9.3%), traction bronchiectasis ($n=7$, 9.3%), consolidation ($n=3$, 4%) and intralobular reticular opacity ($n=3$, 4%) (Figures 1–4).

By contrast, of the 26 patients with elevated KL-6 levels, architectural distortion (Figures 2 and 3) was observed in all cases, followed by nodules (Figures 2–4), interlobular septal thickening and traction bronchiectasis ($n=25$, 96.2%; Figures 2 and 3), bronchial wall thickening ($n=21$, 80.8%; Figure 3), ground-glass opacity ($n=16$, 61.5%; Figure 1) and consolidation ($n=2$, 7.7%, Figure 4).

Ground-glass opacity, nodules, interlobular septal thickening, traction bronchiectasis, architectural distortion and bronchial wall thickening were significantly more frequent in patients with elevated KL-6 levels than in those with normal KL-6 levels ($p<0.001$, $p<0.005$, $p<0.001$, $p<0.001$, $p<0.001$ and $p<0.001$, respectively).

Lymph nodes and effusions

In 70 of 75 patients with normal KL-6 levels (93.3%) and in 21 of 26 patients with elevated KL-6 levels (80.8%), enlarged lymph nodes were observed at the

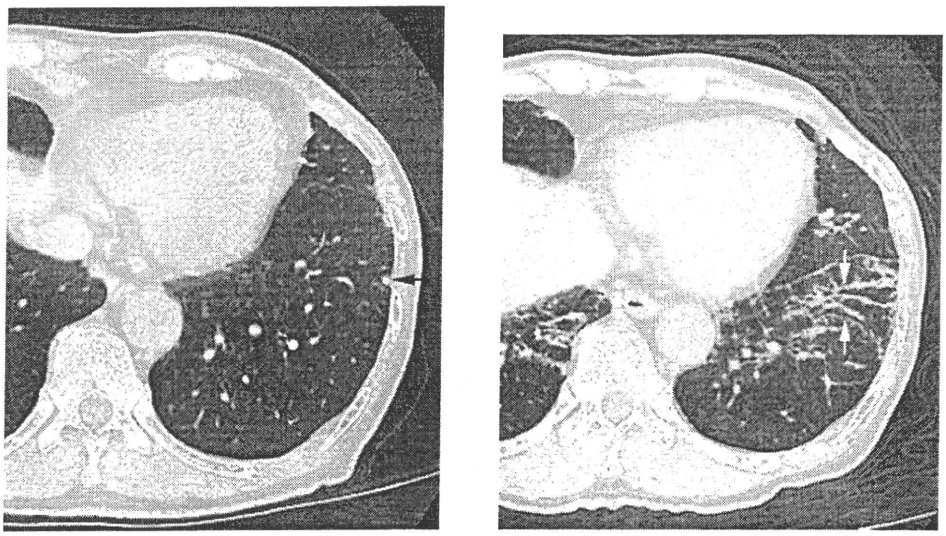

(a) (b)

Figure 2. Image in a 69-year-old man. (a) Transverse CT scan (1 mm section thickness) obtained at the level of left lower lobe shows a nodule in the periphery (arrow; KL-6, 333 U ml^{-1}). (b) Transverse CT scan (1 mm section thickness) obtained 6 months later shows architectural distortion (KL-6, 581 U ml^{-1}). Traction bronchiectasis is also present (arrows).

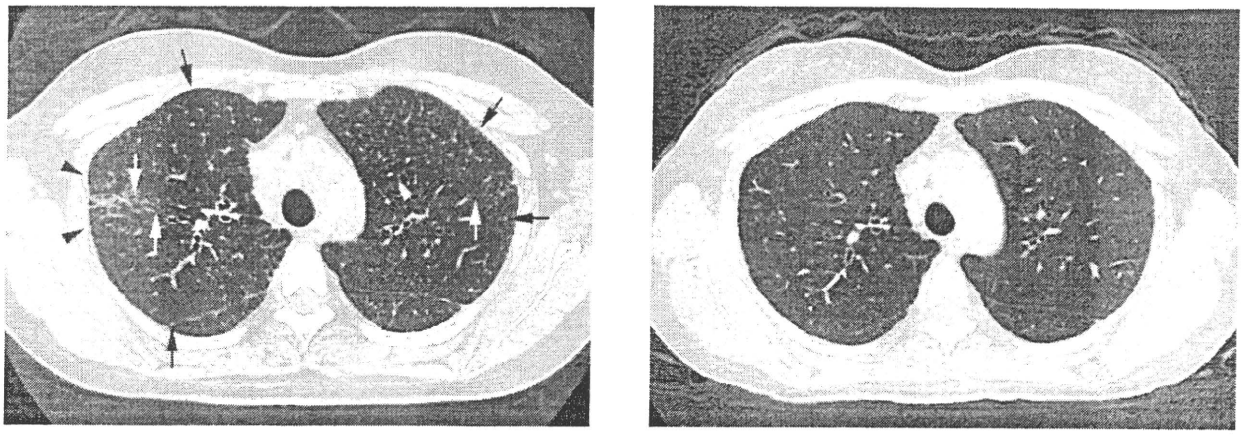

(a) (b)

Figure 3. Images in a 35-year-old woman. (a) Transverse CT scan (1 mm section thickness) obtained at the level of upper lobes shows multiple small nodules (arrows) and architectural distortion (arrowheads; KL-6, 1000 U ml^{-1}). Traction bronchiectasis and bronchial wall thickening are also present (white arrows). (b) Transverse CT scan (1 mm section thickness) obtained 6 months later demonstrates disappearance of nodules, architectural distortion, traction bronchiectasis and bronchial wall thickening (KL-6, 285 U ml^{-1}).

pre-tracheal, paratracheal, tracheobronchial or subcarinal regions (Figure 5). There was no significant difference in frequency of lymph node enlargement between the two groups.

Pleural effusions were not found in any patients in the study.

Follow-up study

Follow-up CT scans were obtained from 36 out of 101 patients at intervals of 1–61 months after initial CT examination (mean follow-up time 7 months). Of 14 patients with ground-glass attenuation (2 patients with normal KL-6 levels and 12 patients with elevated KL-6 levels), follow-up CT scans revealed complete clearing in 1 patient, a decrease in another patient, an increase in 1 patient and no change in 11 patients. In the patients with complete clearing and decreased ground-glass opacity, elevated KL-6 levels improved to within normal limits (Figure 1). In all of the patients with unchanged findings, initial KL-6 levels remained unchanged. By comparison, in the patient with an increase in ground-glass opacity, the KL-6 level worsened.

Of 19 patients with architectural distortion (2 with normal KL-6 levels and 17 with elevated KL-6 levels), follow-up CT scans showed a decrease in 4 patients, no change in 14 patients and an increase in 1 patient. In all patients with improved findings, KL-6 levels decreased (Figure 3); in the patient with worsened findings, the KL-6 level increased (Figure 2).

Of 33 patients with nodules (16 with a normal KL-6 level and 17 with elevated KL-6 levels), follow-up CT scans showed a decrease in 9 patients, no change in 19 patients and an increase in 5 patients. Of the 9 patients with improved findings, KL-6 levels improved in 7

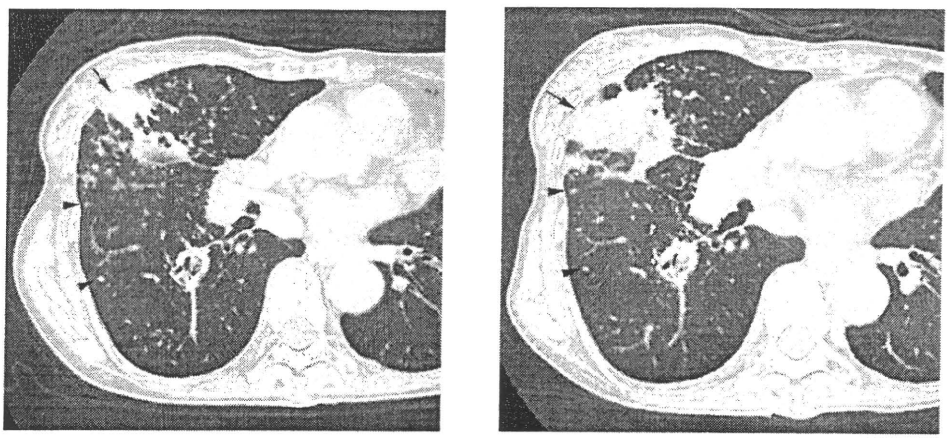

(a) (b)

Figure 4. Images in a 65-year-old woman. (a) Transverse CT scan (1 mm section thickness) obtained at the level of division of right B6 shows consolidation in right middle lobe (arrow) and multiple nodules (arrowheads; KL-6, 400 U ml^{-1}). (b) Transverse CT scan (1 mm section thickness) obtained 5 months later shows worsened consolidation (arrow) and unchanged nodules (arrowheads); however, the KL-6 level is not elevated (KL-6, 397 U ml^{-1}).

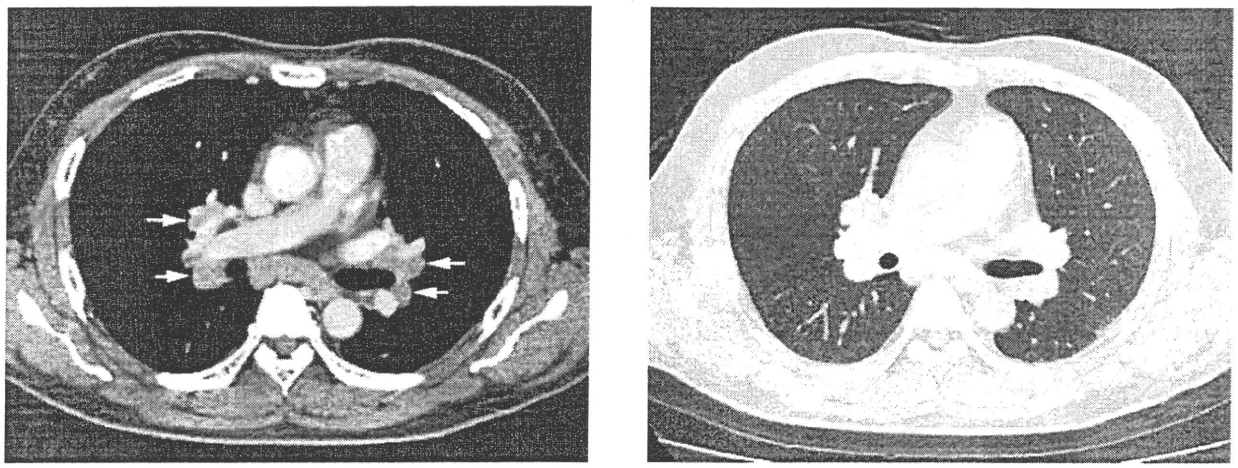

(a) (b)

Figure 5. Images in a 46-year-old male (KL-6, 239 U ml^{-1}) (a) Transverse CT scan (1 mm section thickness) obtained at the level of the right pulmonary artery shows enlarged lymph nodes at subcarinal and bilateral hilar regions (arrows). (b) Transverse CT scan (1 mm section thickness) obtained at the level of the right pulmonary artery shows no abnormal parenchymal lesions.

patients (Figure 3) and remained unchanged in 2. Of the 19 patients with unchanged findings, KL-6 levels improved in 4 patients, remained unchanged in 14 and worsened in 1. By comparison, of the 5 patients with worsened findings, KL-6 levels remained unchanged in 4 and worsened in 1.

Of 22 patients with bronchial wall thickening (8 with normal KL-6 levels and 14 with elevated KL-6 levels), follow-up CT scans showed a decrease in wall thickening in 2 patients, no change in 19 patients and an increase in 1 patient. Of the patients with improved findings, KL-6 levels improved in 1 patient (Figure 3) and remained unchanged in 1. In all of the 19 patients with unchanged findings, initial KL-6 levels remained unchanged. In the patient with an increase in bronchial wall thickening, the KL-6 level worsened.

Of 3 patients with consolidation (2 with normal KL-6 levels and 1 with an elevated KL-6 level), follow-up CT scans remained unchanged in 2 and worsened in 1. In all of the patients with unchanged findings or worsened findings (Figure 4), the initial KL-6 level remained unchanged.

Of 28 patients with lymph node enlargement (15 with normal KL-6 levels and 13 with elevated KL-6 levels), follow-up CT scans showed a decrease in 1 patient and no change in 27 cases. In the patient with improved findings, the KL-6 level improved. Of the 27 patients with unchanged findings, KL-6 levels improved in 13 patients with ameliorated parenchymal abnormalities and worsened in 3 patients with exacerbated parenchymal findings. No change was observed in 11 patients with unchanged parenchymal abnormalities.

Discussion

KL-6 is a mucin-like high molecular weight glycoprotein found in 1988 by Kohno et al [6]. This group also developed a monoclonal antibody against KL-6, which reacts with a sialylated carbohydrate antigen strongly expressed in Type II alveolar pneumocytes and bronchiolar epithelial cells, but not on granulomatous tissue. Several studies demonstrate that KL-6 is elevated in the bronchoalveolar lavage fluid and serum of patients with various types of interstitial pneumonia. The elevation of serum KL-6 levels is considered to be associated with increased permeability of the alveolar capillary barrier [20]. It has also been reported that KL-6 induces chemotaxis of human fibroblasts *in vitro*, suggesting that it may have a pathological role in fibrosing lung disease [21]. Therefore, measurement of serum KL-6 is now widely accepted as a diagnostic marker for monitoring the activity of interstitial lung diseases, such as idiopathic interstitial pneumonia, and for the long-term management of various interstitial diseases [1, 2, 7–11, 13].

The clinical picture of sarcoidosis varies from that of a totally asymptomatic patient, with incidental radiographic findings of bilateral hilar lymphadenopathy, to a seriously dyspnoeic patient with acute respiratory distress syndrome. Alveolitis and subsequent granulomatous processes are important in the pathogenesis of sarcoidosis [22–24]. Bronchoalveolar lavage studies have revealed that the alveolitis in sarcoidosis is characterised by lymphocytic infiltration of T helper cells. The activated T cells release various cytokines such as interleukin-2 and interferon-gamma, which are believed to play many important roles in the pathogenesis of sarcoidosis. Active alveolitis is often accompanied by pulmonary tissue injury or clinical deterioration.

In 1989, Kohno et al [1] reported that serum KL-6 levels were elevated in 4 of 31 patients with sarcoidosis; however, further study was not performed. Kobayashi et al [16] investigated the use of serum KL-6 as a marker for sarcoidosis activity in 47 patients, and found that serum KL-6 levels were significantly elevated in radiographic Type II and Type III patients compared with Type 0 and Type I cases. These observations are similar to those in our study. However, it was difficult to ascertain whether the pulmonary lesions in these patients were characterised by interstitial, granulomatous or fibrous changes.

Hiroshige et al [25] presented a case report of a sarcoidosis patient with an elevated serum KL-6 level, where CT images showed panlobular ground-glass opacity with mosaic distribution. After steroid treatment the CT findings improved and serum KL-6 normalised.

However, no studies describing the radiological findings comparing thin-section CT images between patients with elevated KL-6 levels and those with normal KL-6 levels have been published in English. We retrospectively identified 101 patients with sarcoidosis who underwent chest thin-section CT examinations and had serum KL-6 measured.

Ground-glass opacity, traction bronchiectasis, architectural distortion, nodules, interlobular septal thickening and bronchial wall thickening were significantly more frequent in patients with elevated KL-6 levels than those with normal ones.

Pathologically, ground-glass opacity is considered to represent interstitial inflammatory infiltrate with marked thickening of alveolar septa by fibrous tissue [26]. Lynch et al [27] and Hiroshige et al [25] reported that ground-glass opacities correlated with active diffuse alveolitis.

Traction bronchiectasis and architectural distortion are considered to represent the organisation and fibrosis of the lungs around the bronchi [26, 28]. Our results showed that increased KL-6 levels in sarcoidosis patients whose CT scans consisted of ground-glass attenuation, architectural distortion or traction bronchiectasis may have been caused by an increase in KL-6 production by regenerating alveolar Type II pneumocytes and/or an enhanced permeability following the destruction of the air–blood barrier in the affected lungs.

Bronchial wall thickening, interlobular septal thickening and nodules along bronchi, interlobular septa and pleural regions were also significantly observed more frequently in patients with an elevated KL-6 level than in those with a normal KL-6 level. CT findings are considered to correspond to granulomas, with or without perigranulomatous fibrosis, formed in the connective tissue sheath around the bronchial walls, pulmonary vessels and airways [29]. Thus, our results might be due to perigranulomatous fibrosis with granulomas.

On the other hand, the present study showed that there was no significant difference in the frequency of consolidation between the two groups. Consolidation has revealed alveolitis with inflammatory exudates in alveolar spaces and/or accumulated granulomatous lesions [29–31]. In the present report, biopsy specimens corresponding to consolidation could not be obtained, and whether consolidation shows alveolitis or granulomatous lesions remains unclear. This result may possibly be due to a low frequency of consolidation in this study compared with that of previous studies [31]. Future work should confirm these findings by use of a greater sample size.

Finally, there were several limitations in our study. First, we undertook a retrospective study, and CT image interpretation was performed by consensus. Second, CT findings were not compared with pathological findings in all patients because some patients were asymptomatic and the diagnosis of sarcoidosis could be performed using clinical findings. Third, CT scans, measurement of KL-6 levels and histological specimens were not obtained on the same days. Fourth, CT images were obtained at several CT scans using different protocols. Furthermore, the relationship between the extent of abnormal findings and KL-6 levels was not evaluated.

In summary, thin-section CT findings of nodules, bronchial wall thickening, ground-glass opacity, traction bronchiectasis and architectural distortion were associated with elevated serum KL-6 levels. These results suggest that serum KL-6 levels may be a useful marker for indicating the severity of parenchymal sarcoidosis.

References

1. Kohno N, Kyoizumi S, Awaya Y, Fukuhara H, Yamakido M, Akiyama M. New serum indicator of interstitial pneumonitis activity: sialylated carbohydrate antigen KL-6. Chest 1989;96:68–73.
2. Kobayashi J, Kitamura S. KL-6: A serum marker for interstitial pneumonia. Chest 1995;108:311–15.
3. Ogawa Y, Ishikawa T, Ikeda K, Nakata B, Sawada T, Ogisawa K, et al. Evaluation of serum KL-6, a mucin-like glycoprotein, as a tumor marker for breast cancer. Clin Cancer Res 2000;6:4069–72.
4. Kohno N, Inoue Y, Hamada H, Fujioka S, Fujino S, Yokoyama A, et al. Difference in sero-diagnostic values among KL-6-associated mucins classified as cluster 9. Int J Cancer 1994;8 (Suppl):81–3.
5. Takahashi T, Takamura K, Sakaue S, Ishii J, Yokouchi H, Nasuhara Y. Elevated serum KL-6 concentrations in patients with diabetes mellitus. J Diabetes Complications 2002;16:352–8.
6. Kohno N, Akiyama M, Kyoizumi S, Hakoda M, Kobuke K, Yamakido M. Detection of soluble tumor-associated antigens in sera and effusions using novel monoclonal antibodies, KL-3 and KL-6, against lung adenocarcinoma. Jpn J Clin Oncol 1988;18:203–16.
7. Kohno N, Awaya Y, Oyama T, Yamakido M, Akiyama M, Inoue Y, et al. KL-6, a mucin-like glycoprotein, in bronchoalveolar lavage fluid from patients with interstitial lung disease. Am Rev Respir Dis 1993;148:637–42.
8. Ishii H, Mukae H, Kadota J, Kaida H, Nagata T, Abe K, et al. High serum concentrations of surfactant protein A in usual interstitial pneumonia compared with non-specific interstitial pneumonia. Thorax 2003;58:52–7.
9. Okada F, Ando Y, Honda K, Tanoue S, Matsumoto S, Mori H. Comparison of pulmonary CT findings and serum KL-6 levels in patients with cryptogenic organizing pneumonia. Br J Radiol 2009;82:212–18.
10. Yokoyama A, Kondo K, Nakajima M, Matsushima T, Takahashi T, Nishimura M, et al. Prognostic value of circulation KL-6 in idiopathic pulmonary fibrosis. Respirology 2006;11:164–8.
11. Lin FC, Chen YC, Chang SC. Clinical importance of bronchoalveolar lavage fluid and blood cytokines, surfactant protein D, and Kerbs von Lungren 6 antigen in idiopathic pulmonary alveolar proteinosis. Myyo Clin Proc 2008;83:1344–9.
12. Hant FN, Ludwicka-Bradley A, Wang HJ, Li N, Elashoff R, Tashkin DP, et al. Scleroderma Lung Study Research Group. Surfactant protein D and KL-6 as serum biomarkers of interstitial lung disease in patients with scleroderma. J Rheumatol 2009;36:773–80.
13. Satoh H, Kurishima K, Ishikawa H, Ohtsuka M. Increased levels of KL-6 and subsequent mortality in patients with interstitial lung diseases. J Intern Med 2006;260:429–34.
14. Kitaichi N, Ariga T, Kase S, Yoshida K, Namba K, Ohno S. Usefulness of quantifying serum KL-6 levels in the follow-up of uveitic patients with sarcoidosis. Graefes Arch Clin Exp Ophthalol 2006;244:433–7.
15. Janssen R, Sato H, Glutters JC, Bernard A, van Velzen-Blad H, du Bois RM, et al. Study of Clara cell 16, KL-6, and

surfactant protein-D in serum as disease markers in pulmonary sarcoidosis. Chest 2003;124:2119–25.
16. Kobayashi J, Kitamura S. Serum KL-6 for the evaluation of active pneumonitis in pulmonary sarcoidosis. Chest 1996; 109:1276–82.
17. Statement on sarcoidosis: joint statement of the American Thoracic Society (ATS), the European Respiratory Society (ERS) and the World Association of Sarcoidosis and Other Granulomatous Disorders (WASOG) adopted by the ATS Board of Directors and by the ERS Executive Committee, February 1999. Am J Respir Crit Care Med 1999;160:736–55.
18. Webb WR, Muller NL, Naidich DP. High-resolution computed tomography findings of lung disease. In: Aughenbaugh GL, ed. High-resolution CT of the lung, 3rd edn. Philadelphia, PA: Lippincott Williams & Wilkins, 2001: 71–192.
19. Austin JH, Muller NL, Friedman PJ, Hansell DM, Naidich DP, Remy-Jardin M, et al. Glossary of terms for CT of the lungs: recommendations of the Nomenclature Committee of the Fleischner Society. Radiology 1996;200:327–31.
20. Inoue Y, Barker E, Daniloff E, Hohno N, Hiwada K, Newman S. Pulmonary epithelial cell injury and alveolar-capillary permeability in berylliosis. Am J Respir Crit Care Med 1997;156:109–15.
21. Hirasawa Y, Kohno N, Yokoyama A, Inoue Y, Abe M, Hiwada K. KL-6, a human MUC1 mucin, is chemotactic for human fibroblasts. Am J Respir Cell Mol Biol 1997;17:501–7.
22. Foley NM, Coral AP, Tung K, Hudspith BN, James DG, Johnson NM. Bronchoalveolar lavage cell counts as a predictor of short outcome in pulmonary sarcoidosis. Thorax 1989;44:732–8.
23. Maycock RL, Bertrand P, Morrison CE, Scott JH. Manifestation of sarcoidosis: analysis of 145 patients, with a review of nine series selected from the literature. Am J Med 1963;35:67–89.
24. Israel HL. Prognosis of sarcoidosis. Ann Intern Med 1970;73:1038–9.
25. Hiroshige S, Ando M, Okubo F, Ueno T, Fukami T, Takenaka R, et al. A case of pulmonary sarcoidosis demonstration Panlobular ground-glass opacity with mosaic distribution. Nihon Kokyuki Gakkai Zasshi 2009;47:212–17.
26. Remy-Jardin M, Giraud F, Remy J, Copin MC, Gosselin B, Duhamel A. Importance of ground-glass attenuation in chronic diffuse infiltrative lung disease: pathologic-CT correlation. Radiology 1993;189:693–8.
27. Lynch DA, Webb WR, Gamsu G, Stubarg M, Golden J. Computed tomography in pulmonary sarcoidosis. J Comput Assist Tomogr 1989;13:405–10.
28. Westcott JL, Cole SR. Traction bronchiectasis in end-stage pulmonary fibrosis. Radiology 1986;161:665–9.
29. Nishimura K, Itoh H, Kitaichi M, Nagai S, Izumi T. Pulmonary sarcoidosis: correlation of CT and histopathologic findings. Radiology 1993;189:105–9.
30. Nakano Y, Kurihara N, Miyamoto O, Takamatus K, Adachi N, Fujiwara H, et al. A case of sarcoidosis beginning with extensive ground-glass pattern on chest X-ray, accompanied with high fever and eosinophilia. Nihon Kyobu Shikkan Gakkai Zasshi 1989;27:98–106.
31. Abehsera M, Veleyre D, Grenier P, Jaillet H, Battesti JP, Brauner MW. Sarcoidosis with pulmonary fibrosis: CT patterns and correlation with pulmonary function. AJR Am J Roentgenol 2000;174:1751–7.

Respirology

ORIGINAL ARTICLE

Osteopontin levels are elevated in patients with eosinophilic pneumonia

TAKUYA UENO,[1] EISHI MIYAZAKI,[2] MASARU ANDO,[1] SHIN-ICHI NUREKI[1] AND TOSHIHIDE KUMAMOTO[1]

[1]*Department of Internal Medicine 3,* and [2]*Center for Community Medicine, Faculty of Medicine, Oita University, Oita, Japan*

ABSTRACT

Background and objective: **Osteopontin is a key cytokine involved in pro-inflammatory T helper type 1 (Th1)-associated immune responses, which has recently been implicated in allergic diseases. We investigated the pathogenic role of osteopontin in eosinophilic pneumonia.**

Methods: **The concentrations of osteopontin and Th1- or Th2-associated cytokines were measured in BAL fluid (BALF) from 41 patients with eosinophilic pneumonia, including those with acute (AEP, $n = 12$), chronic (CEP, $n = 16$), or drug-induced eosinophilic pneumonia (DEP, $n = 13$). The results were compared with those from patients with other interstitial lung diseases. Immunocytochemistry and double immunofluorescence labelling were performed to determine the cellular source of osteopontin.**

Results: **Osteopontin was significantly elevated in BALF from patients with eosinophilic pneumonia as compared with BALF from patients with drug-induced interstitial pneumonia, hypersensitivity pneumonitis, idiopathic interstitial pneumonia, or sarcoidosis, and also compared with BALF from healthy volunteers. Osteopontin concentrations elevated at the time of exacerbation decreased during clinical improvement, either spontaneously or as a result of corticosteroid therapy. Elevated concentrations of CXCL10, CCL17 and IL-10 were also detected in BALF from patients with eosinophilic pneumonia. Osteopontin concentrations in BALF of AEP patients were correlated with IL-5, as well as IL-10, CCL11, CCL17 and CXCL10 concentrations. In AEP and DEP patients, serum osteopontin concentrations were also elevated. Double immunofluorescence labelling showed that in patients with eosinophilic pneumonia, osteopontin was expressed in lung eosinophils.**

Conclusions: **Osteopontin is likely to contribute to the development of inflammation in patients with eosinophilic pneumonia.**

Key words: cytokine, eosinophil, interstitial lung disease, osteopontin, pneumonia.

SUMMARY AT A GLANCE

Osteopontin concentrations were considerably elevated in BAL fluid of patients with eosinophilic pneumonia, and osteopontin was expressed at high levels in lung eosinophils. There was a strong correlation between osteopontin and IL-5 levels in acute eosinophilic pneumonia. Osteopontin may contribute to the development of eosinophilic pneumonia.

INTRODUCTION

Osteopontin is a secreted phosphorylated acidic glycoprotein that contains the arginine-glycine-aspartic acid (RGD) integrin-binding domain commonly found in matrix proteins.[1] Osteopontin has functions in various physiological and pathological processes, including bone remodelling, maintenance or reconfiguration of tissue integrity during inflammatory processes, tumour cell metastasis, and cell-mediated immunity.[1–3] Previous studies have shown that osteopontin contributes to the development of Th1-mediated immunity and Th1-associated diseases.[2] Increased levels of osteopontin have been observed in various Th1-associated lung diseases, including sarcoidosis[4] and tuberculosis.[5] Osteopontin has also recently been implicated in allergic diseases. Elevated levels of osteopontin have been detected in the tear fluid of patients with allergic conjunctival diseases,[6] and in the airways of patients with bronchial asthma,[7,8] or chronic rhinosinusitis with nasal polyps.[9]

Eosinophilic pneumonia is characterized by the accumulation of eosinophils in the lung parenchyma, which can result from several conditions, including allergic reactions to various drugs or fungi,

Correspondence: Eishi Miyazaki, Center for Community Medicine, Oita University Faculty of Medicine, 1-1 Idaigaoka, Hasama-machi, Yufu, Oita 879-5593, Japan. Email: eishida@med.oita-u.ac.jp

Received 29 December 2009; invited to revise 2 February 2010; revised 24 April 2010; accepted 30 May 2010 (Associate Editor: Yuben Moodley).

Respirology (2010) **15**, 1111–1121
doi: 10.1111/j.1440-1843.2010.01825.x

helminthic infections and environmental exposures.[10–12] When these specific causes can be excluded, eosinophilic pneumonia is classified as idiopathic, and this includes chronic eosinophilic pneumonia (CEP)[10,13] and acute eosinophilic pneumonia (AEP).[10,14–20] Unlike CEP, the aetiology of which is usually undetermined, most cases of AEP in Japan occur in association with cigarette smoking.[19,20] AEP can also be clinically and histologically distinguished from CEP;[21] however, both syndromes share several immunological mechanisms that lead to eosinophilic inflammation. In general, eosinophilic pneumonia is characterized by a Th2-polarized condition, with increased levels of the Th2-derived cytokines IL-4, IL-5 and IL-13, as well as the Th2-attracting chemokines thymus- and activation-regulated chemokine (TARC)/CC chemokine ligand (CCL)17, and macrophage-derived chemokine (MDC)/CCL21, in BAL fluid (BALF) of patients.[22–25] However, the roles of osteopontin, as well as the Th1-associated chemokine interferon-inducing protein-10/CXCL10, in eosinophilic pneumonia have not yet been elucidated.

In the present study, we investigated the pathogenic role of osteopontin in eosinophilic pneumonia by measuring osteopontin levels in the BALF and serum of patients with various types of eosinophilic pneumonia, including AEP, CEP and drug-induced eosinophilic pneumonia (DEP). In addition, the relationship between BALF osteopontin concentrations and clinical and immunological parameters was analysed. The cellular source of osteopontin was determined by immunocytochemistry and double immunofluorescence labelling.

METHODS

Patients

The study was performed retrospectively with approval from the institutional review board. Forty-one patients with eosinophilic pneumonia, including those with AEP, CEP or DEP, who were treated at the Oita University Hospital or the Shin-Beppu Hospital between January 1995 and July 2007, were included in the study. AEP was diagnosed according to the following criteria: acute febrile illness, bilateral diffuse pulmonary infiltrates, hypoxaemia, an increased percentage of eosinophils in BALF and the absence of possible causes other than smoking. CEP was diagnosed by the following criteria: typical clinical features consistent with CEP (fever, malaise, weight loss, cough, sputum), dense, multiple foci of consolidation in the peripheral lungs, an increased percentage of eosinophils in BALF, the absence of possible causes, and a prompt response to corticosteroid therapy. Attention was paid to the differential diagnosis of allergic bronchopulmonary aspergillosis. Patients with DEP satisfied the following diagnostic criteria: pulmonary eosinophilia >10%, prompt improvement after cessation of the causative drug, the absence of other possible causes, and a positive reaction to lymphocyte stimulation tests or recurrence of the symptoms on challenge with the drug.

The study also included patients with drug-induced interstitial pneumonia (DIP), who met the criteria for DEP but did not show pulmonary eosinophilia. In addition, patients with hypersensitivity pneumonitis, idiopathic interstitial pneumonia or sarcoidosis, as well as healthy volunteers, were included as control subjects. For each of these patients, the diagnosis was established on the basis of standard clinical criteria and histopathological evidence. Patients with malignancies, autoimmune diseases or complicated infectious diseases were excluded because increased circulating levels of osteopontin have been observed in these diseases.[26–29]

BAL

After informed consent was obtained, BAL was performed principally for diagnostic purposes. Briefly, a fibreoptic bronchoscope was placed into a bronchus of the affected lobe, three 50-mL aliquots of saline solution were instilled and the BALF specimens were collected. After determination of the total cell concentration, the cells were placed on slides by cytospin centrifugation at 70 × g for 5 min and stained with May–Grünwald–Giemsa solution for a differential count on 300 cells. The remaining BALF was centrifuged at 5,200 × g for 20 min to remove cells and the supernatants were stored at −80°C until used in the ELISA.

Blood samples

Serum samples were obtained by centrifugation of clotted blood (1500 *g*, 4°C, 10 min), and stored at −80°C until the measurements were performed.

Measurement of osteopontin, cytokines and chemokines

The levels of osteopontin and other cytokines and chemokines were measured using specific, commercially available kits according to the manufacturer's protocol. Osteopontin concentrations were measured using an ELISA kit (IBL, Gunma, Japan), and the concentrations of other cytokines and chemokines were measured using ELISA kits from R&D Systems Inc., Minneapolis, MN, USA. The lower limits of detection for osteopontin, IL-5, IL-10, eotaxin/CCL11, CCL17 and CXCL10 were 3.3 ng/mL, 4.0 pg/mL, 3.9 pg/mL, 5.0 pg/mL, 7.0 pg/mL and 1.7 pg/mL, respectively. For the purposes of statistical analysis, concentrations below the detection limits were assumed to be zero.

Immunocytochemistry for osteopontin

Aliquots of BAL cells (1×10^6 cells) were pelleted onto glass slides and fixed in cold acetone for 10 min. After incubation in a solution containing 1% BSA and 10%

Table 1 Characteristics of the patients with different types of eosinophilic pneumonia and other diffuse inflammatory lung diseases

	Gender male/female	Age (years)	Smoking smokers/ non-smokers	Eosinophils in serum (%)	Asthmatic yes/no	Duration from the onset (days)
AEP	10/2	19 (15–21)**	12/0***	8.9 (0.0–23.6)	3/9	3 (1–7)**
CEP	4/12*	54 (24–79)	5/11	20.0 (14.1–46.6)**	6/10	21 (24–52)
DEP	10/3	66 (26–83)	8/5	6.9 (0.4–40.8)	1/12	5 (3–16)
DIP	6/4	70 (35–79)	4/6	3.8 (0.7–12.4)	0/10	6 (3–17)
HP	4/7	62 (52–82)	4/7	3.7 (1.2–10.1)	1/10	16 (11–24)
IIP	9/6	71 (48–81)	8/7	4.0 (0.6–12.8)	1/14	ND
SAR	10/30*	53 (19–83)	13/27	3.2 (0.8–8.9)	2/38	ND
HV	12/2	25 (21–32)	7/7	—	0/14	—

Data are presented as medians (range) unless indicated otherwise.

* $P < 0.001$ compared with the HV group (chi-square test); ** $P < 0.05$ compared with the other groups (Mann–Whitney *U*-test); *** $P < 0.05$ compared with the other groups (chi-square test).

AEP, acute eosinophilic pneumonia; CEP, chronic eosinophilic pneumonia; DEP, drug-induced eosinophilic pneumonia; DIP, drug-induced interstitial pneumonia; HP, hypersensitivity pneumonitis; HV, healthy volunteer; IIP, idiopathic interstitial pneumonia; ND, not determined; SAR, sarcoidosis.

normal goat serum, the specimens were incubated for 2 h at room temperature with a 1:5000 dilution of rabbit anti-human osteopontin polyclonal antibody (PoAb; Thermo Scientific, Fremont, CA, USA). Negative controls were incubated with rabbit IgG at the same concentration as the primary antibody. After blocking endogenous peroxidase activity by incubation in a solution of 0.3% H_2O_2 (Wako Pure Chemical Industries, Osaka, Japan) and 0.1% NaN_3 for 30 min, the bound antibodies were labelled with biotin-conjugated goat anti-rabbit IgG. Avidin-biotin-peroxidase complex (Vector Laboratories, Burlingame, CA, USA) was applied for 30 min and peroxidase activity was visualized by incubation with amino-3, 9-ethylcarbazole for 10 min. The sections were counter-stained with Mayer's haematoxylin and mounted with Aquatex (Merck KGaA, Darmstadt, Germany).

Double immunofluorescence labelling

For double immunofluorescence, 1×10^6 BAL cells were pelleted onto glass slides and fixed in 4% paraformaldehyde for 10 min. The fixed cells were treated with 0.5% Triton-X (Sigma-Aldrich, St Louis, MO, USA) in PBS for 15 min. After blocking endogenous peroxidase activity by incubation in a solution of 3% BSA in 0.1% Triton-X/PBS for 20 min, the slides were incubated with a 1:25 dilution of rabbit anti-human osteopontin PoAb and a mouse anti-human major basic protein (MBP) mAb (Millipore, Billerica, MA, USA) or a mouse anti-human integrin-α4 (9F10) mAb (Santa Cruz Biotechnology, Santa Cruz, CA, USA), at the same dilution, at room temperature for 2 h. After washing three times with 0.1% Triton-X/PBS, the slides were stained for 2 h at room temperature with an Alexa-Fluor 488 $F(ab')_2$-labelled fragment of goat anti-rabbit IgG for detection of osteopontin or with an Alexa-Fluor 568 $F(ab')_2$-labelled fragment of goat anti-mouse IgG (Molecular Probes, Invitrogen, Carlsbad, CA, USA), both diluted 1:100, for detection of MBP and integrin-α4. Alternatively, the specimens were labelled with anti-osteopontin PoAb followed by Alexa-Fluor 488 $F(ab')_2$ fragment of goat anti-rabbit IgG, and then incubated with 50 μg/mL of propidium iodide (Sigma-Aldrich) to visualize nuclei. Images were captured by confocal microscopy (Carl Zeiss, Inc., Oberkochen, Germany).

Statistical analyses

Data are presented as median values with the ranges. The Kruskal–Wallis test was used to compare the values for the different groups. If there were significant differences between the groups, inter-group differences were assessed for statistical significance using the non-parametric Mann–Whitney *U*-test. Differences in the characteristics of the study populations were assessed using the chi-square test for nominal data and Student's *t*-test for continuous data. Changes in osteopontin levels during evolution of the disease within the same individual were assessed using the Wilcoxon signed rank test. Spearman's correlation coefficient was used to assess potential correlations between variables. *P*-values < 0.05 were considered statistically significant.

RESULTS

Patient characteristics and BAL profiles

The characteristics of the study population are shown in Table 1. The eosinophilic pneumonia group included 24 male patients and 17 female patients. The median age was 52 years (range 15–83). Twelve patients met the criteria for AEP, 16 met the criteria for CEP, and 13 met the criteria for DEP. The patients in

Table 2 Cellular profile of BAL from patients with different types of eosinophilic pneumonia and other diffuse inflammatory lung diseases

	Recovery (%)	Cell count ($\times 10^5$/mL)	Eosinophils (%)	Lymphocytes (%)	Neutrophils (%)
AEP	53.3 (30.0–70.0)*	10.0 (3.3–86.1)*	50.1 (26.4–86.4)**	18.2 (5.9–34.3)*	2.8 (0.0–5.5)
CEP	38.7 (28.7–63.3)*	6.5 (1.2–25.0)*	47.8 (14.0–93.0)**	5.0 (0.5–38.0)	1.8 (0.0–13.4)
DEP	46.2 (26.6–73.3)*	4.3 (1.5–9.0)*	26.4 (11.7–33.7)**	27.4 (5.2–56.3)*	4.0 (0.0–40.0)
DIP	45.6 (33.3–61.1)*	5.4 (0.7–21.4)*	5.0 (0.0–9.0)	21.9 (13.0–79.0)*	3.3 (0.0–64.0)
HP	40.8 (30.0–63.3)*	12.1 (6.2–32.9)*	0.0 (0.0–6.2)	72.2 (52.0–83.7)*	12.5 (8.8–25.2)*
IIP	33.3 (23.3–63.3)*	1.4 (0.8–3.5)	2.3 (1.0–8.2)	12.2 (4.1–62.2)	4.5 (1.0–11.2)*
SAR	51.3 (33.3–80.0)*	2.4 (1.0–7.2)*	0.0 (0.0–1.0)	23.8 (31.3–96.3)*	0.5 (0.0–1.6)
HV	62.0 (53.3–74.7)	1.5 (0.8–2.4)	0.2 (0.0–4.7)	5.4 (1.3–9.5)	1.2 (0.0–2.8)

Data are presented as medians (range).

* $P < 0.05$ compared with the HV group (Mann–Whitney *U*-test);

** $P < 0.001$ compared with the DIP, HP, IIP, SAR and HV groups (Mann–Whitney *U*-test).

AEP, acute eosinophilic pneumonia; CEP, chronic eosinophilic pneumonia; DEP, drug-induced eosinophilic pneumonia; DIP, drug-induced interstitial pneumonia; HP, hypersensitivity pneumonitis; HV, healthy volunteer; IIP, idiopathic interstitial pneumonia; SAR, sarcoidosis.

the AEP group tended to be younger than those in the other groups. All patients with AEP were current smokers. The percentage of peripheral blood eosinophils was significantly higher in the CEP group than in the other groups. Three patients with AEP had previous histories of bronchial asthma; however, none of these individuals had asthma symptoms at the time of presentation. Six patients with CEP and one patient with DEP had current symptoms of bronchial asthma. None of the patients with DIP, hypersensitivity pneumonitis, idiopathic interstitial pneumonias or sarcoidosis had current symptoms of asthma. All patient samples were obtained at the time of diagnosis, and none of the patients was undergoing treatment with corticosteroids or other immunomodulatory drugs at the time of sampling.

The BAL cell profile is summarized in Table 2. BAL cell numbers were significantly increased in the AEP, CEP, DEP, DIP, hypersensitivity pneumonitis and sarcoidosis groups as compared with the control group. The percentages of BAL eosinophils were significantly higher in the AEP, CEP and DEP groups compared with the other groups. All patients, except those in the CEP group, showed increased percentages of lymphocytes in BAL as compared with the control group. The AEP, hypersensitivity pneumonitis and idiopathic interstitial pneumonia patients had more BAL neutrophils compared with the control group.

Osteopontin concentrations in BALF

Osteopontin was detected in unconcentrated BALF from all patients with eosinophilic pneumonia. The osteopontin concentrations in BALF of patients with eosinophilic pneumonia were significantly higher than those in BALF of patients with DIP, hypersensitivity pneumonitis, idiopathic interstitial pneumonia, or sarcoidosis, and also compared with those in healthy control subjects (Fig. 1a). However, there was no significant difference in BALF osteopontin concentrations between the different groups of eosinophilic pneumonia patients, and interestingly, patients with DEP had significantly higher osteopontin concentrations compared with those with DIP (Fig. 1b).

The influence of incident asthma on the BALF osteopontin concentrations was investigated. There were no significant differences in the BALF osteopontin concentrations between all asthmatic and all non-asthmatic subjects, or between the asthmatic and non-asthmatic subjects within the eosinophilic pneumonia group. Similarly, the patients with AEP were all smokers; however, there were no differences in BALF osteopontin concentrations between smokers and non-smokers.

CXCL10, CCL17 and IL-10 concentrations in BALF

To understand the immunological characteristics of AEP, CEP and DEP, CXCL10, CCL17 and IL-10 levels were measured in BALF. CXCL10 levels were significantly higher in patients with AEP, CEP or DEP, and in sarcoidosis patients when compared with healthy volunteers (Fig. 2a). There were no differences in BALF CXCL10 levels among AEP, CEP and DEP patients.

All but three of the 41 patients with eosinophilic pneumonia had detectable concentrations of CCL17 in their BALF, whereas CCL17 was detected in only one of the 12 healthy volunteers and in none of the 40 sarcoidosis patients. BALF CCL17 concentrations were significantly higher in patients with AEP, CEP or DEP than in patients with sarcoidosis or healthy volunteers (Fig. 2b). These results are consistent with previously published data.[23]

Detectable IL-10 concentrations were present in BALF from 25 of 38 patients with eosinophilic pneumonia, whereas IL-10 was detected in BALF from only two healthy volunteers and was not detected in BALF from sarcoidosis patients. BALF IL-10 concentrations were significantly higher in patients with AEP, CEP or

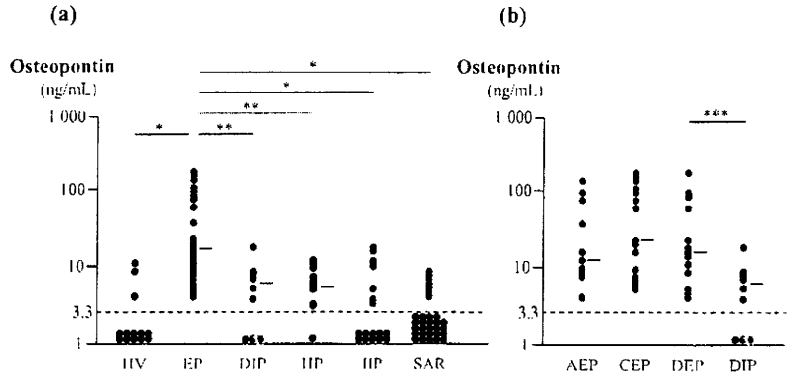

Figure 1 (a) Osteopontin concentrations in BAL fluid from healthy volunteers (HV) and patients with eosinophilic pneumonia (EP), drug-induced interstitial pneumonia (DIP), hypersensitivity pneumonitis (HP), idiopathic interstitial pneumonia (IIP) or sarcoidosis (SAR). The EP group was subdivided into patients with acute eosinophilic pneumonia (AEP), chronic eosinophilic pneumonia (CEP) or drug-induced eosinophilic pneumonia (DEP). (b) Comparison of osteopontin concentrations in BAL fluid of patients with AEP, CEP, DEP or DIP. Osteopontin concentrations are plotted on a log scale, with the short horizontal lines indicating the median values. The detection limits of the assay are indicated by the horizontal dashed line. $*P < 0.0001$, $**P < 0.001$, $***P < 0.05$ (Mann–Whitney *U*-test).

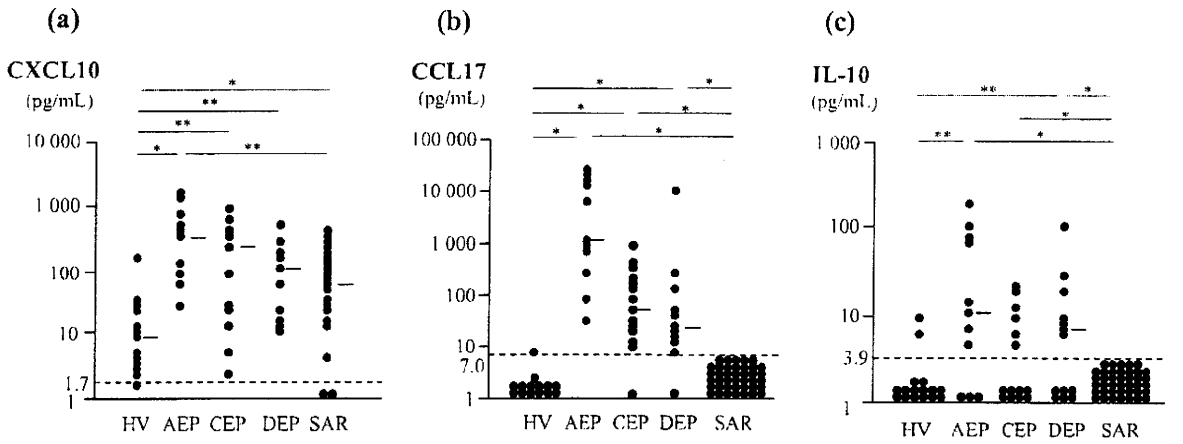

Figure 2 The concentrations of (a) CXCL10, (b) CCL17 and (c) IL-10 in BAL fluid of healthy volunteers (HV) and patients with acute eosinophilic pneumonia (AEP), chronic eosinophilic pneumonia (CEP), drug-induced eosinophilic pneumonia (DEP) or sarcoidosis (SAR). The concentrations are plotted on a log scale, with the short horizontal lines indicating the median values. The detection limits of the assays are indicated by the horizontal dashed lines. $*P < 0.0001$, $**P < 0.005$ (Mann–Whitney *U*-test).

DEP than in sarcoidosis patients (Fig. 2c). There were no differences in BALF IL-10 levels among the different groups of eosinophilic pneumonia patients.

Changes in osteopontin concentrations during the clinical course of eosinophilic pneumonia

Ten patients with eosinophilic pneumonia underwent a second BAL approximately 17 days (range 11–43 days) after the initial examination. Six of these patients were being treated with corticosteroids. The elevated BALF concentrations of osteopontin observed at the time of the first BAL had decreased, in parallel with clinical improvement, by the time of the second BAL (Fig. 3).

Osteopontin levels were correlated with CRP, IL-5, IL-10, CCL11, CCL17 and CXCL10 levels in patients with acute eosinophilic pneumonia

The correlations of BALF osteopontin concentrations with several biomarkers, including cytokines and chemokines were examined in patients with AEP. There was a significant correlation between BALF osteopontin concentrations and serum CRP levels, which reflect the degree of inflammation and may be

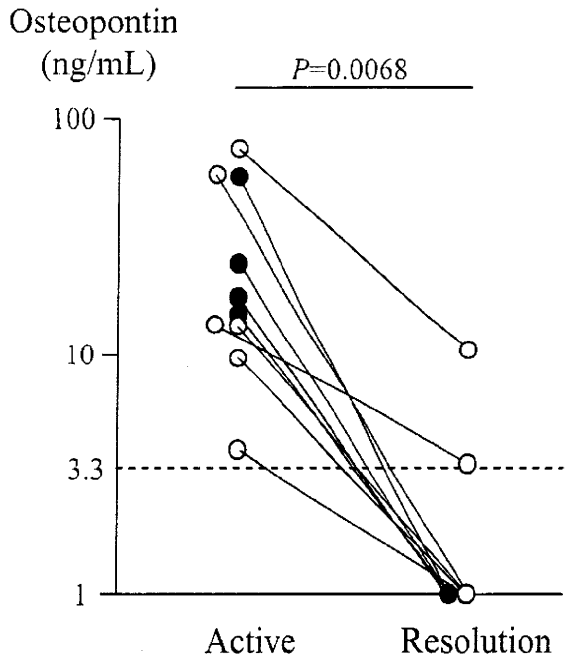

Figure 3 Osteopontin concentrations in BAL fluid obtained at the active and resolution phases of the disease in 10 patients with eosinophilic pneumonia, including three with acute eosinophilic pneumonia, four with chronic eosinophilic pneumonia, and four with drug-induced eosinophilic pneumonia. Six patients received corticosteroid therapy (open circles) and the remaining four patients showed spontaneous resolution (closed circles). Osteopontin concentrations are plotted on a log scale. The detection limit of the osteopontin assay is indicated by the horizontal dashed line.

indicative of disease activity (Fig. 4a). BALF osteopontin concentrations were also significantly correlated with the concentrations of CXCL10, IL-5 and CCL11 in the BALF of patients with AEP (Fig. 4b–d). In addition, there were positive correlations between osteopontin and IL-10 ($P = 0.0086$, $r = 0.876$), as well as CCL17 concentrations ($P = 0.0498$, $r = 0.618$).

Circulating osteopontin levels

Circulating osteopontin concentrations were significantly higher in patients with AEP or DEP than in healthy control subjects (Fig. 5); however, osteopontin measurements did not enable patients with eosinophilic pneumonia to be distinguished from healthy controls. Elevated serum osteopontin levels were also observed in sarcoidosis patients. There was a significant correlation between the BALF and serum osteopontin concentrations in sarcoidosis patients, but not in patients with eosinophilic pneumonia.

Expression of osteopontin in BAL cells

Immunocytochemistry was performed to detect osteopontin in BAL cells from patients with eosinophilic pneumonia or sarcoidosis, as well as healthy volunteers. Negative controls incubated with an irrelevant isotype-matched Ig were uniformly non-reactive. Osteopontin expression was detected on cells with glass-shaped nuclei in BALF from patients with eosinophilic pneumonia (Fig. 6a), but not from patients with sarcoidosis or healthy volunteers. Osteopontin expression was also observed in most large mononuclear cells obtained from patients with eosinophilic pneumonia (Fig. 6a) or sarcoidosis (Fig. 6b), as well as those from healthy volunteers (Fig. 6c).

Phenotype of osteopontin-positive cells

Double immunofluorescence labelling was performed to determine the phenotype of osteopontin-positive cells in BALF. Double immunofluorescence labelling with an osteopontin antibody and propidium iodide showed that most of the osteopontin-positive cells possessed glass-shaped nuclei (Fig. 6d–f). Double immunofluorescence labelling with antibodies to osteopontin and MBP or integrin-α4, as eosinophil markers, showed co-expression of osteopontin and MBP by the same BAL cells (Fig. 6g–i). Similarly, BAL cells co-expressed osteopontin and integrin-α4, which is a component of very late antigen-α4 (Fig. 6j–l).

DISCUSSION

The present study is the first to report increased concentrations of osteopontin in BALF of patients with eosinophilic pneumonia. The BALF osteopontin levels in patients with eosinophilic pneumonia were significantly higher than those in patients with other types of diffuse inflammatory lung diseases. BALF osteopontin levels were increased in active disease and decreased during the patient's clinical improvement. Osteopontin levels were closely correlated with IL-5 and CCL11 levels in the BALF of patients with AEP. Double immunofluorescence labelling showed that osteopontin was expressed in lung eosinophils in the BALF of patients with eosinophilic pneumonia. These findings suggest that osteopontin plays a role in the pathogenesis of eosinophilic pneumonia.

Serial examination of BAL in 10 patients with eosinophilic pneumonia showed that osteopontin concentrations decreased dramatically in parallel with clinical improvement. At the time of the second BAL, six patients were receiving corticosteroid treatment. Hayami *et al.* showed that dexamethasone treatment induced an increase in osteopontin expression.[29] However, Kirton *et al.* have shown that dexamethasone treatment reduced the expression of osteopontin.[30] The present results are consistent with the observations of Kurokawa *et al.*, who showed an inhibitory effect of corticosteroids on osteopontin production in a murine model of allergic asthma.[31] The present study also showed that BALF osteopontin concentrations were significantly correlated with serum CRP levels, an indication of disease activity, in

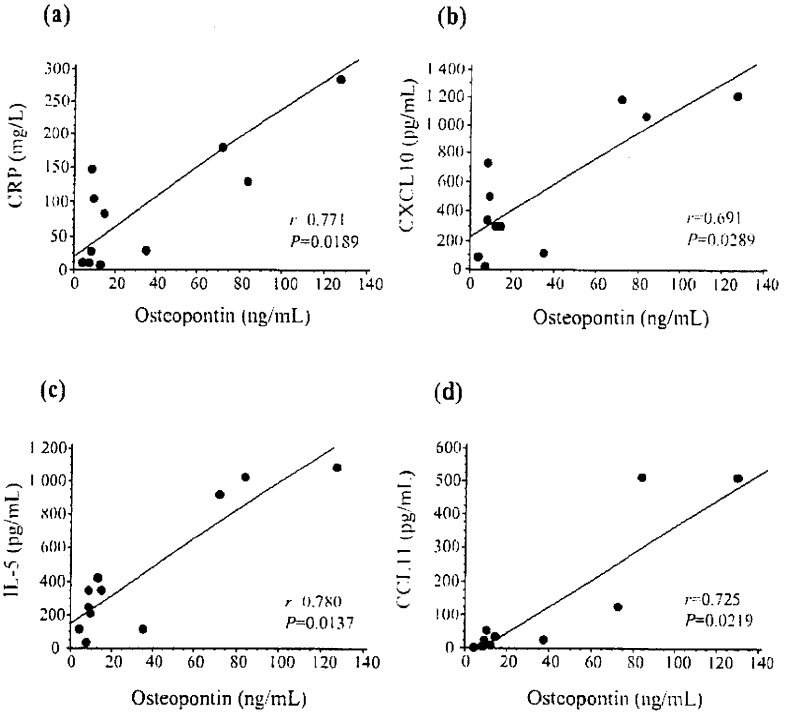

Figure 4 Correlations between (a) BAL fluid osteopontin and serum CRP conentrations, and between osteopontin and (b) CXCL10, (c) IL-5 and (d) CCL11 concentrations in BAL fluid from patients with acute eosinophilic pneumonia. The 95% CI for the correlations between osteopontin and CRP, CXCL10, IL-5 and CCL11 were $0.3301 < \rho < 0.9288$, $0.1941 < \rho < 0.9057$, $0.2588 < \rho < 0.9173$, and $0.3733 < \rho < 0.9357$, respectively.

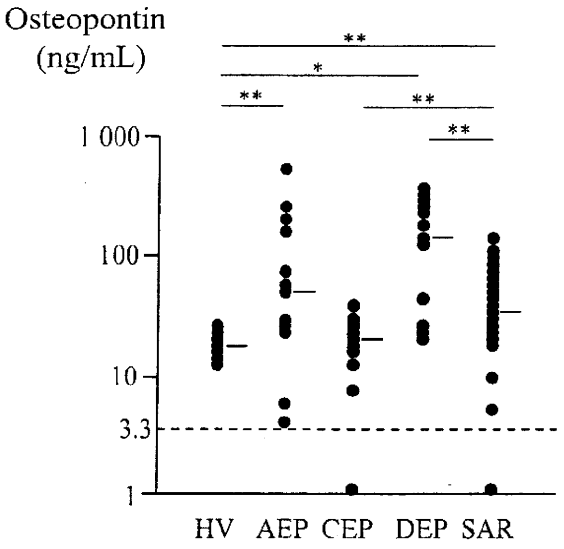

Figure 5 Serum osteopontin concentrations in healthy volunteers (HV) and patients with acute eosinophilic pneumonia (AEP), chronic eosinophilic pneumonia (CEP), drug-induced eosinophilic pneumonia (DEP) or sarcoidosis (SAR). Osteopontin concentrations are plotted on a log scale, with the short horizontal lines indicating the median values. The detection limit for osteopontin is indicated by the horizontal dashed line. $*P < 0.001$, $**P < 0.05$ (Mann–Whitney *U*-test).

patients with AEP. These results suggest that osteopontin plays a pathogenic role in eosinophilic pneumonia, and that corticosteroids may regulate osteopontin expression.

Although increased concentrations of osteopontin in serum or plasma have been reported in several inflammatory conditions, infectious diseases and malignancies,[26–28] few studies have measured osteopontin levels in BALF. Previous studies have documented high levels of osteopontin expression in Th1-mediated granulomatous lung diseases, such as sarcoidosis[4] and tuberculosis.[5] In the present study, osteopontin levels were higher in patients with eosinophilic pneumonia than in those with sarcoidosis or hypersensitivity pneumonitis. In addition, elevation of BALF osteopontin concentrations was independent of the clinical type of eosinophilic pneumonia, suggesting that elevated osteopontin levels may be a universal feature of the pathophysiology of eosinophilic inflammation and pneumonia. Furthermore, comparison of BALF osteopontin levels in different drug-induced lung diseases categorized according to the presence of BALF eosinophilia showed that osteopontin concentrations were significantly higher in patients with DEP than in those with DIP. These results suggested a relationship between osteopontin levels and pulmonary eosinophilia.

Double immunofluorescence labelling was performed to assess the co-expression of osteopontin and eosinophil markers in the same cells obtained by BAL. The results showed that the osteopontin-positive cells in the BALF of patients with eosinophilic pneumonia were eosinophils and macrophages. This observation is consistent with previous studies

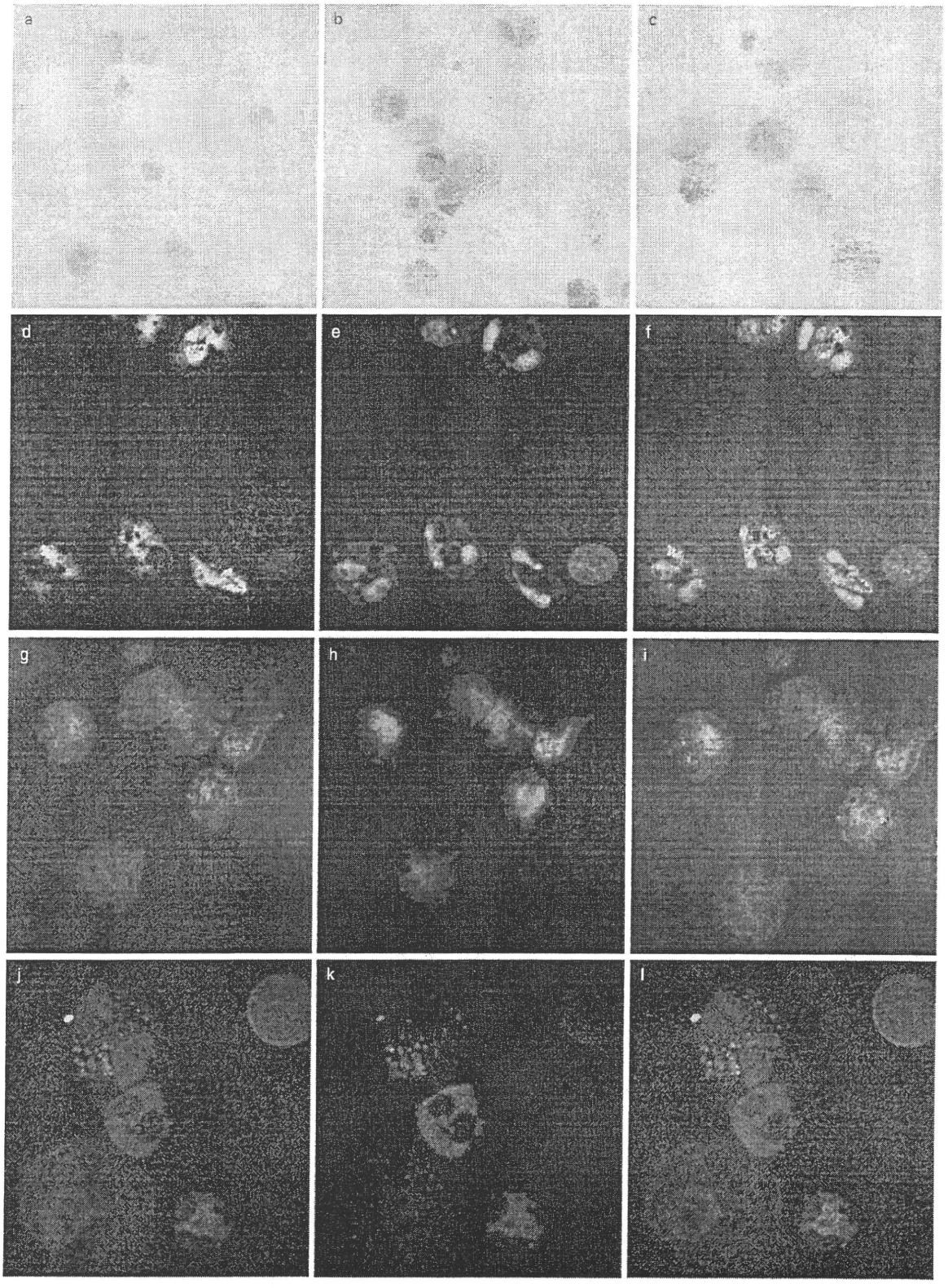

Figure 6 Immunocytochemical (a–c) and double immunofluorescence labelling (d–l) of BAL cells from healthy volunteers and patients with eosinophilic pneumonia or sarcoidosis, using specific antibodies for osteopontin, major basic protein (MBP) and integrin-α4. Representative results are shown. (a) Most cells with glass-shaped nuclei were positive for osteopontin in a patient with acute eosinophilic pneumonia (AEP). (b) Mononuclear cells from a patient with sarcoidosis, and (c) from a healthy volunteer were positive for osteopontin. (d), (g) and (j) Immunofluorescence labelling for osteopontin in BAL cells harvested from a patient with AEP (green). Co-labelling with (e) propidium iodide, (h) anti-MBP antibody and (k) anti-integrin-α4 antibody is indicated in red. (f) The merged images show osteopontin expression in cells with glass-shaped nuclei; (i) colocalization of osteopontin with MBP and (l) colocalization of osteopontin with integrin-α4 (yellow). (e) Cells labelled with integrin-α4 were osteopontin-positive, and (l) a cell that was only positive for osteopontin was also observed.

showing that osteopontin is expressed by tissue eosinophils infiltrating into nasal polyps,[9] and located in the peribronchial inflammatory infiltrate of asthma patients.[7] Given the large numbers of eosinophils in the BALF of patients with eosinophilic pneumonia, lung eosinophils are likely to be the major source of osteopontin at sites of inflammation. The present study was unable to clarify whether other cells, such as injured epithelium and vascular endothelium in the inflamed lungs of patients with eosinophilic pneumonia,[1,32] contribute to the production and increased levels of osteopontin in BALF.

Given that accumulation of eosinophils in the lungs is thought to be a major factor in the pathogenesis of eosinophilic pneumonia, and that eosinophil-derived proteins are likely to cause lung injury, attention has recently focused on the mechanisms of eosinophil recruitment to the lungs. In this context, the Th2-associated cytokines, IL-4, IL-5 and IL-13, and the Th2-attracting chemokines, CCL17, CCL22 and CCL11, participate in eosinophilic inflammation by upregulating Th2-type immune responses.[22–25,33] In the present study, osteopontin levels were closely correlated with the levels of IL-5 and CCL11 in BALF of patients with AEP. Recently, osteopontin was shown to induce IL-5 production in the sino-nasal mucosa of patients with chronic rhinosinusitis,[9] and Puxeddu *et al.* showed that IL-5 increased osteopontin expression in human eosinophils.[34] In addition, recent studies showed close correlations between osteopontin concentrations and the numbers of tissue eosinophils,[9,34] while *in vitro* studies showed that osteopontin promoted eosinophil chemotaxis.[34,35] Therefore, the cycle of eosinophilic inflammation may be amplified due to induction of osteopontin by IL-5 and the recruitment and activation of eosinophils by osteopontin.

In the present study, CXCL10, CCL17 and IL-10 concentrations were measured in BALF of patients with eosinophilic pneumonia or sarcoidosis. The chemokine and cytokine BALF concentrations were higher in eosinophilic pneumonia than in sarcoidosis. CXCL10 is a specific ligand for CXCR3 on Th1 cells; this chemokine is therefore thought to be important in Th1-mediated immune responses.[36,37] Kato *et al.* have previously shown increased CXCL10 concentrations in BALF of patients with CEP,[38] although there was no increase in CXCR3-expressing $CD4^+$ T lymphocytes. Therefore, CXCL10 may have alternative functions in eosinophilic pneumonia. It has been reported that CXCR3 is also expressed on Th2 cells,[39] and that when these Th2 cells are activated, they are recruited to the airways in response to CXCL10.[40,41] Human peripheral blood eosinophils are also reported to migrate in response to the CXCR3 ligands.[42] The present study showed that IL-10 was detectable in over half the patients with eosinophilic pneumonia, whereas osteopontin was undetectable in all patients with sarcoidosis, suggesting that IL-10 may be more important in eosinophilic pneumonia. IL-10 is an anti-inflammatory Th2 cytokine, and a recent *in vitro* study showed that IL-10 induced osteopontin expression in dendritic cells.[43] Further studies are required to clarify the functional link between IL-10 and eosinophil-derived osteopontin.

Serum osteopontin levels were also measured in patients with eosinophilic pneumonia or sarcoidosis. Serum osteopontin levels were higher in sarcoidosis patients than in control subjects, which is in keeping with the results of previous studies.[5,44] Serum osteopontin concentrations were also elevated in patients with AEP or DEP; however, osteopontin levels could not be used to distinguish between patients with eosinophilic pneumonia and healthy control subjects. Because BALF protein is estimated to be 100 times less concentrated than that of the alveolar lining fluid,[45] the ratio of osteopontin in BALF to that in serum appeared to be high in patients with eosinophilic pneumonia. This indicated that osteopontin is mainly generated in the inflamed lungs of patients with eosinophilic pneumonia. However, osteopontin production in granulomatous lesions at sites other than the lungs may contribute to the elevation of serum osteopontin in sarcoidosis patients.

The present study was performed retrospectively at a single institution. Given the low incidence of eosinophilic pneumonia, sera that had been stored at −80°C were used for the measurement of osteopontin. Although osteopontin may be less stable in serum than in plasma, preliminary experiments showed a good correlation between the osteopontin concentrations measured in serum and plasma. Serum osteopontin levels have been used as a diagnostic or prognostic biomarker in malignancies.[46,47] However, there were only small numbers of patients in each of the eosinophilic pneumonia groups. To avoid these limitations, a prospective multicentre study is required.

The increased generation of osteopontin by lung eosinophils may be crucial to the development of

eosinophilic pneumonia. The present study showed wide variations in osteopontin levels in BALF and serum from patients with eosinophilic pneumonia, and this may be associated with the strength of Th2 responses, as well as the clinical course and other undetermined factors. Further studies are warranted to define the exact role of osteopontin in lung inflammation in patients with eosinophilic pneumonia.

ACKNOWLEDGEMENTS

The authors are grateful to Dr Kenichiro Nakamura, Ms Mariko Ono and Ms Kaori Hirano, Department of Internal Medicine 3, Faculty of Medicine, Oita University, for their valuable technical assistance.

REFERENCES

1 Denhardt DT, Noda M, O'Regan AW *et al.* OPN as a means to cope with enviromental insults: regulation of inflammation, tissue remodeling, and cell survival. *J. Clin. Invest.* 2001; **107**: 1055–61.
2 O'Regan AW, Nau GJ, Chupp GL *et al.* Osteopontin (Eta-1) in cell-mediated immunity: teaching an old dog new tricks. *Immunol. Today* 2000; **21**: 475–8.
3 Ashkar S, Weber GF, Panoutsakopoulou V *et al.* Eta-1 (osteopontin): an early component of type-1 (cell-mediated) immunity. *Science* 2000; **287**: 860–4.
4 O'Regan AW, Chupp GL, Lowry JA *et al.* Osteopontin is associated with T cells in sarcoid granulomas and has T cell adhesive and cytokine-like properties in vitro. *J. Immunol.* 1999; **162**: 1024–31.
5 Koguchi Y, Kawakami K, Uezu K *et al.* High plasma osteopontin level and its relationship with interleukin-12-mediated type 1 T helper cell response in tuberculosis. *Am. J. Respir. Crit. Care Med.* 2003; **167**: 1355–9.
6 Uchio E, Matsuura N, Kadonosono K *et al.* Tear osteopontin levels in patients with allergic conjunctival diseases. *Graefes. Arch. Clin. Exp. Ophthalmol.* 2002; **240**: 924–8.
7 Kohan M, Bader R, Puxeddu I *et al.* Enhanced osteopontin expression in a murine model of allergen-induced airway remodelling. *Clin. Exp. Allergy* 2007; **37**: 1444–54.
8 Xanthou G, Alissafi T, Semitekolou M *et al.* Osteopontin has a crucial role in allergic airway disease through regulation of dendritic cell subsets. *Nat. Med.* 2007; **13**: 570–8.
9 Lu X, Zhang XH, Wang H *et al.* Expression of osteopontin in chronic rhinosinusitis with and without nasal polyps. *Allergy* 2009; **64**: 104–11.
10 Allen J, Davis W. The eosinophilic lung diseases. *Am. J. Respir. Crit. Care Med.* 1994; **150**: 1423–38.
11 Cooper JA Jr, White DA, Matthay RA. Drug-induced pulmonary disease. Part 2: Noncytotoxic drugs. *Am. Rev. Respir. Dis.* 1986; **133**: 488–505.
12 Rom WN, Weiden M, Garcia R *et al.* Acute eosinophilic pneumonia in a New York City firefighter exposed to World Trade Center dust. *Am. J. Respir. Crit. Care Med.* 2002; **166**: 797–800.
13 Carrington CB, Addington WW, Goff AM *et al.* Chronic eosinophilic pneumonia. *N. Engl. J. Med.* 1969; **280**: 787–98.
14 Allen JN, Pacht ER, Gadek JE *et al.* Acute eosinophilic pneumonia as a reversible cause of noninfectious respiratory failure. *N. Engl. J. Med.* 1989; **321**: 569–74.
15 Badesch D, King TJ, Schwarz M. Acute eosinophilic pneumonia: a hypersensitivity phenomenon? *Am. Rev. Respir. Dis.* 1989; **139**: 249–52.
16 Allen J. Acute eosinophilic pneumonia. *Semin. Respir. Crit. Care Med.* 2006; **27**: 142–7.
17 Philit F, Etienne-Mastroïanni B, Parrot A *et al.* Idiopathic acute eosinophilic pneumonia: a study of 22 patients. *Am. J. Respir. Crit. Care Med.* 2002; **166**: 1235–9.
18 Pope-Harman AL, Davis WB, Allen ED *et al.* Acute eosinophilic pneumonia. A summary of 15 cases and review of the literature. *Medicine (Baltimore)* 1996; **75**: 334–42.
19 Uchiyama H, Suda T, Nakamura Y *et al.* Alterations in smoking habits are associated with acute eosinophilic pneumonia. *Chest* 2008; **133**: 1174–80.
20 Shintani H, Fujimura M, Ishiura Y *et al.* A case of cigarette smoking-induced acute eosinophilic pneumonia showing tolerance. *Chest* 2000; **117**: 277–9.
21 Mochimaru H, Kawamoto M, Fukuda Y *et al.* Clinicopathological differences between acute and chronic eosinophilic pneumonia. *Respirology* 2005; **10**: 76–85.
22 Walker C, Bauer W, Braun RK *et al.* Activated T cells and cytokines in bronchoalveolar lavages from patients with various lung diseases associated with eosinophilia. *Am. J. Respir. Crit. Care Med.* 1994; **150**: 1038–48.
23 Miyazaki E, Nureki S, Fukami T *et al.* Elevated levels of thymus- and activation-regulated chemokine in bronchoalveolar lavage fluid from patients with eosinophilic pneumonia. *Am. J. Respir. Crit. Care Med.* 2002; **165**: 1125–31.
24 Katoh S, Fukushima K, Matsumoto N *et al.* Accumulation of CCR4-expressing CD4+ T cells and high concentration of its ligands (TARC and MDC) in bronchoalveolar lavage fluid of patients with eosinophilic pneumonia. *Allergy* 2003; **58**: 518–23.
25 Nureki S, Miyazaki E, Ando M *et al.* CC chemokine receptor 4 ligand production by bronchoalveolar lavage fluid cells in cigarette-smoke-associated acute eosinophilic pneumonia. *Clin. Immunol.* 2005; 116.
26 Sennels H, Sørensen S, Ostergaard M *et al.* Circulating levels of osteopontin, osteoprotegerin, total soluble receptor activator of nuclear factor-kappa B ligand, and high-sensitivity C-reactive protein in patients with active rheumatoid arthritis randomized to etanercept alone or in combination with methotrexate. *Scand. J. Rheumatol.* 2008; **37**: 241–7.
27 Chang YS, Kim HJ, Chang J *et al.* Elevated circulating level of osteopontin is associated with advanced disease state of non-small cell lung cancer. *Lung Cancer* 2007; **57**: 373–80.
28 Wong CK, Lit LC, Tam LS *et al.* Elevation of plasma osteopontin concentration is correlated with disease activity in patients with systemic lupus erythematosus. *Rheumatology (Oxford)* 2005; **44**: 602–6.
29 Hayami T, Zhang Q, Kapila Y *et al.* Dexamethasone's enhancement of osteoblastic markers in human periodontal ligament cells is associated with inhibition of collagenase expression. *Bone* 2007; **40**: 93–104.
30 Kirton JP, Wilkinson FL, Canfield AE *et al.* Dexamethasone downregulates calcification-inhibitor molecules and accelerates osteogenic differentiation of vascular pericytes: implications for vascular calcification. *Circ. Res.* 2006; **98**: 1264–72.
31 Kurokawa M, Konno S, Matsukura S *et al.* Effects of corticosteroids on osteopontin expression in a murine model of allergic asthma. *Int. Arch. Allergy Immunol.* 2009; **149**: 7–13.
32 Brown LF, Berse B, Van de Water L *et al.* Expression and distribution of osteopontin in human tissues: widespread association with luminal epithelial surfaces. *Mol. Biol. Cell* 1992; **3**: 1169–80.
33 Katoh S, Matsumoto N, Fukushima K *et al.* Elevated chemokine levels in bronchoalveolar lavage fluid of patients with eosinophilic pneumonia. *J. Allergy Clin. Immunol.* 2000; **106**: 730–6.
34 Puxeddu I, Berkman N, Ribatti D *et al.* Osteopontin is expressed and functional in human eosinophils. *Allergy* 2010; **65**: 168–74.
35 Takahashi A, Kurokawa M, Konno S *et al.* Osteopontin is involved in migration of eosinophils in asthma. *Clin. Exp. Allergy* 2009; **39**: 1152–9.
36 Sallusto F, Lenig D, Mackay CR *et al.* Flexible programs of chemokine receptor expression on human polarized T helper 1 and 2 lymphocytes. *J. Exp. Med.* 1998; **187**: 875–83.

37 Deng W, Ohmori Y, Hamilton TA. Mechanisms of IL-4-mediated suppression of IP-10 gene expression in murine macrophages. *J. Immunol.* 1994; **153**: 2130–6.
38 Katoh S, Fukushima K, Matsumoto N *et al.* Accumulation of CXCR-3-expressing eosinophils and increased concentration of its ligands (IP-10 and Mig) in bronchoalveolar lavage fluid of patients with chronic eosinophilic pneumonia. *Int. Arch. Allergy Immunol.* 2005; **137**: 229–35.
39 Nanki T, Lipsky PE. Lack of correlation between chemokine receptor and T(h)1/T(h)2 cytokine expression by individual memory T cells. *Int. Immunol.* 2000; **12**: 1659–66.
40 Thomas MS, Kunkel SL, Lukacs NW. Differential role of IFN-gamma-inducible protein 10 kDa in a cockroach antigen-induced model of allergic airway hyperreactivity: systemic versus local effects. *J. Immunol.* 2002; **169**: 7045–53.
41 Jinquan T, Jing C, Jacobi HH *et al.* CXCR3 expression and activation of eosinophils: role of IFN-gamma-inducible protein-10 and monokine induced by IFN-gamma. *J. Immunol.* 2000; **165**: 1548–56.
42 Sedgwick JB, Menon I, Gern JE *et al.* Effects of inflammatory cytokines on the permeability of human lung microvascular endothelial cell monolayers and differential eosinophil transmigration. *J. Allergy Clin. Immunol.* 2002; **110**: 752–6.
43 Konno S, Eckman JA, Plunkett B *et al.* Interleukin-10 and Th2 cytokines differentially regulate osteopontin expression in human monocytes and dendritic cells. *J. Interferon Cytokine Res.* 2006; **26**: 562–7.
44 Kadota J, Mizunoe S, Mito K *et al.* High plasma concentrations of osteopontin in patients with interstitial pneumonia. *Respir. Med.* 2005; **99**: 111–17.
45 Rennard S, Basset G, Lecossier D *et al.* Estimation of volume of epithelial lining fluid recovered by lavage using urea as marker of dilution. *J. Appl. Physiol.* 1986; 60.
46 Creaney J, Robinson BW. Serum and pleural fluid biomarkers for mesothelioma. *Curr. Opin. Pulm. Med.* 2009; **15**: 366–70.
47 Isa S, Kawaguchi T, Teramukai S *et al.* Serum osteopontin levels are highly prognostic for survival in advanced non-small cell lung cancer: results from JMTO LC 0004. *J. Thorac. Oncol.* 2009; **4**: 1104–10.